A non-enzymatic function associated with a putative histone demethylase licenses epigenetic inheritance

AUTHORS

Gulzhan Raiymbek[1], Sojin An[1], Nidhi Khurana[1], Saarang Gopinath[1], Raymond Trievel[1,2], Uhn-soo Cho[1,2] and Kaushik Ragunathan[1*]

AFFILIATIONS

[1] Department of Biological Chemistry, University of Michigan, Ann Arbor, MI, USA

[2] Department of Biophysics, University of Michigan, Ann Arbor, MI, USA

***** To whom correspondence should be addressed: ragunath@umich.edu

ABSTRACT

H3K9 methylation (H3K9me) specifies the establishment and maintenance of transcriptionally silent epigenetic states or heterochromatin. The enzymatic erasure of histone modifications is widely assumed to be the primary mechanism that resets epigenetic states during and after DNA replication. Here, we demonstrate that a putative histone-demethylase Epe1 in fission yeast, regulates epigenetic inheritance through a non-enzymatic process. Mutations that map to its putative catalytic domain disrupt its interaction with $Swi6^{HP1}$ and heterochromatin specific pattern of localization without any requirement for enzymatic activity. Epe1 and $Swi6^{HP1}$ form an inhibitory complex which displaces histone deacetylases from sites of heterochromatin formation. Sequence-specific recruitment of a histone deacetylase, Clr3 renders heterochromatin refractory to the anti-silencing functions of Epe1 and licenses the inheritance of epigenetic states in *cis.* Epigenetic inheritance solely depends on the read-write activity of the H3K9 methyltransferase Clr4 which competes with genome-wide nucleosome turnover processes in the absence of enzymatic erasure.

INTRODUCTION

Histone H3 lysine methylation is a conserved mark of transcriptional silencing and is associated with the formation of specialized domains called heterochromatin. Heterochromatin formation is critical for centromere and telomere function, silencing of transposons and repetitive DNA elements and for maintaining lineage-specific patterns of gene expression (Grewal and Jia, 2007; Nicetto et al., 2019). Heterochromatin formation requires sequence-specific establishment factors that direct histone modifiers to distinct sites in the genome (Moazed, 2011). In fission yeast, a major pathway for sequence-specific recruitment of histone modifiers involves the small RNA binding protein Argonaute (Ago1) which directs the H3K9 methyltransferase, Clr4^{Suv39h} to the pericentromeric repeats and the mating type locus (Bayne et al., 2010; Hall et al., 2002; Verdel et al., 2004; Volpe et al., 2002). H3K9 methylation serves as a platform for the binding of a key architectural protein, Swi6^{HP1}. The oligomerization of Swi6^{HP1} creates a scaffold that subsequently recruits diverse chromatin modifiers to sites of heterochromatin formation. These include proteins that play important roles in the context of DNA replication, transcriptional silencing and centromere assembly (Fischer et al., 2009).

Once established, H3K9me spreads through a mechanism that depends on the read-write activity of Clr4^{Suv39h}. Two conserved, structural attributes of Clr4^{Suv39h} enable this process: a conserved chromodomain that recognizes and binds to H3K9me and a SET domain that is responsible for catalysis. This ability of Clr4^{Suv39h} to bind to the product of its own enzymatic activity enables the silencing of genes that are distant from heterochromatin nucleation centers (Al-Sady et al., 2013; Zhang et al., 2008). In addition to heterochromatin spreading, read-write mechanisms are also indispensable during the maintenance of epigenetic states following DNA replication (Zhang et al., 2008). Modified histones that are partitioned between daughter DNA strands serve as templates to mark newly deposited histones. This H3K9 methylation-centric positive feedback loop sustains the sequence-independent inheritance of silent epigenetic states during mitosis and meiosis (Audergon et al., 2015; Ragunathan et al., 2015). The regulation of heterochromatin spreading and inheritance impinges on the activity of a putative histone demethylase, Epe1. The loss of Epe1 leads to increased heterochromatin spreading beyond normal boundary sequences, the inheritance of H3K9 methylation via sequence-independent pathways, increased cell to cell variation in H3K9 methylation patterns and the acquisition of adaptive epigenetic traits (Audergon et al., 2015; Ayoub et al., 2003; Ragunathan et al., 2015; Wang et al., 2015; Zofall and Grewal, 2006; Zofall et al., 2012). Hence, Epe1 is directly involved in antagonizing heterochromatin associated processes that explicitly depend on the read-write activity of Clr4^{Suv39h}. Despite its critical role in heterochromatin regulation, the molecular basis for how Epe1 exerts its anti-silencing functions in cells remains largely unknown (Trewick et al., 2007).

Epe1 most closely resembles JumonjiC (JmjC) domain containing proteins that utilize iron and α-ketoglutarate as co-factors to demethylate post-translationally modified lysine and arginine residues (Tsukada et al., 2006). Histone demethylases have prominent roles in regulating the reversibility of epigenetic states (Iwase et al., 2007; Whetstine et al., 2006). Unlike active histone demethylases where an HxD/E….H motif is involved in Fe (II) coordination, Epe1 has a non-canonical HXE….Y motif (Tsukada et al., 2006). Structural studies of an Epe1 ortholog, PHF2 suggest that this non-conserved and naturally occurring histidine to tyrosine substitution results in a low affinity iron binding state that could impair its catalytic functions (Horton et al., 2011). Although Epe1 bears a strong resemblance to histone demethylases at the amino acid level, there is no biochemical evidence to support the notion that Epe1 harbors any enzymatic histone demethylase activity. Epe1 purified from fission yeast cells, or a recombinant source (insect cells) does not exhibit H3K9 demethylase activity *in vitro* when H3K9me nucleosomes are used as substrates (Tsukada et al., 2006; Zofall and Grewal,

2006). Despite this lack of biochemical evidence, genetic studies in fission yeast reveal an indispensable role for amino acid residues involved in co-factor binding. The mutation of residues involved in Fe (II) and α-ketoglutarate binding leads to H3K9 methylation spreading beyond normal heterochromatin boundaries resembling cells that completely lack Epe1 (Trewick et al., 2007). These contrasting lines of biochemical and genetic data have prompted several alternative explanations for how Epe1 might exert its anti-silencing function in cells. This includes the possibility that Epe1 acts as a protein hydroxylase which targets non-histone proteins such as Swi6^{HP1}, disrupts the assembly and activity of the multi-subunit H3K9 methyltransferase CLRC complex, or functions as an H3K9 demethylase in complex with the HP1 homolog, Swi6^{HP1} (Aygun et al., 2013; Iglesias et al., 2018; Trewick et al., 2007; Zofall and Grewal, 2006). Although these models present attractive possibilities for how Epe1 regulates heterochromatin formation, there is no direct evidence to suggest that any of these proteins represent bonafide enzymatic targets.

Epe1 is recruited to sites of heterochromatin formation through its interactions with Swi6^{HP1}. This recruitment process is regulated via two distinct and non-overlapping mechanisms. First, Epe1 protein levels are regulated in a cell cycle dependent manner through the activity of a Cul4-Ddb1 E3 ubiquitin ligase. Preventing the proteasomal degradation of Epe1 leads to its increased occupancy at sites of heterochromatin formation which is also accompanied by a defect in transcriptional silencing (Braun et al., 2011). A second mechanism that regulates Epe1 recruitment is the casein kinase II (*ckb1*) dependent phosphorylation of Swi6^{HP1}. Eliminating Swi6^{HP1} phosphorylation leads to the loss of transcriptional gene silencing, increased occupancy of Epe1 at pericentromeric repeat regions and a corresponding decrease in the recruitment of key heterochromatin regulators such as the histone deacetylase, Clr3 (Shimada et al., 2009). Despite these correlations, we do not understand if changes in Swi6^{HP1} dependent protein-protein interactions are sufficient to alter heterochromatin stability and whether these functions explicitly require the enzymatic or non-enzymatic functions of Epe1.

The establishment and maintenance of epigenetic states is primarily thought to depend on a balance of enzymatic activities between readers, writers and erasers of histone modifications (Allis and Jenuwein, 2016). However, the replication dependent and independent turnover of histones serves as a major mechanism that shapes genome wide-patterns of histone methylation (Chory et al., 2019). In *Drosophila*, nucleosome turnover mechanisms may act as fundamental limitations to histone modifications serving as carriers of epigenetic memory (Coleman and Struhl, 2017; Deal et al., 2010; Laprell et al., 2017). In principle, passive genome-wide nucleosome exchange processes can compete with histone modification dependent read-write activities to attenuate the inheritance of silent epigenetic states. In fission yeast, Epe1 and the histone deacetylase Clr3 have opposing effects on nucleosome turnover (Aygun et al., 2013). These observations raise the possibility that Epe1 could potentially have a direct role in stimulating nucleosome exchange. However, we lack any mechanistic insight into how the JmjC domain of Epe1 can participate in modulating genome-wide nucleosome turnover or if these heterochromatin specific functions of Epe1 require its putative enzymatic activity.

In this study, we discovered an unexpected non-enzymatic function associated with Epe1. Mutations that affect co-factor binding within the JmjC domain of Epe1 disrupt a direct, biochemical interaction between Epe1 and Swi6^{HP1}. We show that these alterations in biochemical interactions between the two proteins is independent of any enzymatic activity. We propose that Epe1 forms an inhibitory complex with Swi6^{HP1} which disrupts heterochromatin assembly and the formation of this complex is dependent both on co-factor binding and H3K9 methylation. We find that Epe1 has a direct role in displacing histone deacetylases such as Clr3 from sites of heterochromatin formation. We propose that the recruitment of histone deacetylases creates a chromatin environment that is permissive to the read-write activity of

Clr4^{Suv39h} enabling silent epigenetic states to be propagated amidst an epigenome that is in a state of constant flux.

RESULTS

Mutations that affect co-factor binding disrupt the interaction between Epe1 and Swi6^{HP1}

Epe1 resembles JumonjiC (JmjC) domain containing histone demethylases. These enzymes leverage iron (Fe (II)) and α-ketoglutarate (α-KG) as co-factors to catalyze the oxidative demethylation of modified lysine residues (Tsukada et al., 2006). Aligning primary amino acid sequences of active histone demethylases and Epe1 reveals a histidine to tyrosine substitution within a conserved Fe (II) binding site (**Figure 1A**). We tested whether this distal, non-conserved iron binding residue in the case of Epe1 (Y370) is essential for its function in cells. We used a reporter gene assay where a TetR-Clr4 fusion protein is recruited to an ectopic site where ten Tet operator sites (*10X TetO*) are placed upstream of a reporter gene, *ade6*$^{+}$ (**Figure 1B**). The silencing of the *ade6*$^{+}$ reporter causes cells to turn red on low adenine containing medium whereas gene activation leads to the appearance of white colonies. Red or sectored colonies are observed in the presence of tetracycline only in cells that lack a functional copy of Epe1 either by deletion or mutation (Audergon et al., 2015; Ragunathan et al., 2015). Consistent with previous reports, the expression of Epe1 mutants (*epe1 H297A and epe1 Y307A*) that are defective in Fe (II) and α-KG binding leads to a loss of Epe1 function. Cells are red on medium lacking tetracycline and display a sectored appearance on +tetracycline containing medium (**Figure 1C**). We observed the same phenotype upon replacing the non-conserved tyrosine residue that is unique to Epe1 with alanine (*epe1 Y370A*) wherein cells exhibit a sectored appearance on +tetracycline containing medium. We measured the expression levels of all Epe1 mutants using a FLAG antibody relative to actin. The expression levels of the different Epe1 alleles we tested was similar to that of the endogenous protein suggesting that neither overexpression artifacts nor changes in protein stability contribute to the phenotypes we observed (**Supplementary Figure 1A**). We used chromatin immunoprecipitation assays followed by qPCR to measure H3K9me2 levels associated with the reporter gene locus before and after the addition of tetracycline. Cells exhibit high levels of H3K9me2 in the absence of tetracycline consistent with the establishment of epigenetic silencing (**Figure 1D**). Upon tetracycline addition, H3K9me2 persists only in cells that lack a functional allele of Epe1 indicating maintenance of the epigenetic state on +tetracycline containing medium (**Figure 1E**). Our genetic assays reveal that the non-conserved tyrosine residue (Y370) is essential for Epe1 activity in the context of epigenetic inheritance.

Epe1 co-factor binding mutants, when over-expressed, phenocopy wild-type cells in terms of their capacity to silence reporter genes and rescue *epe1Δ* strains (Trewick et al., 2007; Zofall and Grewal, 2006). One plausible mechanism is that Epe1 co-factor binding mutants do not properly localize to sites of heterochromatin formation and the overexpression of these mutants overcomes this localization defect. The primary mechanism of Epe1 recruitment to sites of heterochromatin formation is through its interactions with the HP1 homolog, Swi6^{HP1}. We used co-immunoprecipitation assays to first test whether the wild-type Epe1 protein and co-factor binding mutants interact equally with Swi6^{HP1}. We constructed C-terminal 3X FLAG tag fusions of all Epe1 variants for these assays which are expressed from the endogenous locus. Although the wild-type Epe1 protein exhibits a significant interaction with Swi6^{HP1}, every single Epe1 mutant that is defective in co-factor binding exhibits a concomitant loss of interaction with Swi6^{HP1} (**Figure 1F**). These results suggest that point mutations within the catalytic domain of Epe1 alter its ability to interact with the HP1 homolog, Swi6^{HP1}. We confirmed that the position of the epitope tag in the case of Epe1 does not alter our conclusions. An N-terminal 3X FLAG tag fusion of Epe1 qualitatively resemble co-immunoprecipitation experiments performed using C-terminal 3X FLAG tag fusions of Epe1. A point mutation within co-factor binding residues leads

to the loss of a biochemical interaction between Epe1 and Swi6^{HP1} (**Supplementary Figure 1B**).

Given that the interaction between Epe1 and Swi6^{HP1} is important for its heterochromatin specific pattern of localization, we tested whether this loss of interaction between the two proteins leads to its reduced occupancy at sites of heterochromatin formation. We used formaldehyde crosslinking of cells followed by chromatin immunoprecipitation (ChIP-qPCR) using a FLAG antibody to measure Epe1 protein levels at sites of heterochromatin formation. Epe1 mutants that are non-functional in our genetic assays exhibit reduced heterochromatin occupancy and their levels are similar to cells that completely lack H3K9 methylation (*clr4Δ*) or the HP1 homolog, Swi6 (*swi6Δ*) (**Figure 1G)**. Altering crosslinking conditions to more sensitively capture transient chromatin dependent interactions did not alter the conclusions of our experiments (**Supplementary Figure 1C**). Hence, co-factor binding mutations in Epe1 have two major consequences: 1) a loss of interaction with Swi6^{HP1} 2) a complete inability to localize to sites of heterochromatin formation. It is noteworthy that these molecular defects directly correlate with a loss of Epe1 function in cells (**Figure 1C**).

In vitro binding assays reveal a direct role for the JmjC domain in regulating the interaction between Epe1 and Swi6^{HP1}

There are two possible models can explain our observations 1) a mutation within the JmjC domain alters the conformation of Epe1 leading to the loss of its interaction with Swi6^{HP1} (non-enzymatic) 2) the catalytic activity of Epe1 is essential for binding to Swi6^{HP1} implying that demethylation is coupled to a protein-protein interaction (enzymatic). To test whether mutations within the JmjC domain directly affect protein-protein interactions, we expressed and purified maltose binding protein (MBP) fusions of wild type Epe1 (Epe1 WT) and an Epe1 mutant (Epe1 H297A) from insect cells and also separately purified recombinant 3XFLAG- Swi6^{HP1} from *E.coli*. We verified that Epe1 is soluble before and after cleaving the MBP tag using TEV protease (**Supplementary Figure 2A**). Due to limiting amounts of recombinant Epe1 following our purifications, we used western blots to measure the interaction between Epe1 and Swi6^{HP1}. We immobilized 3X-FLAG- Swi6^{HP1} on FLAG antibody beads maintaining a fixed amount of Swi6^{HP1} throughout the course of our binding assays. We then added increasing amounts of either wild-type MBP-Epe1 or MBP-Epe1 H297A and measured their interaction with Swi6^{HP1}. Consistent with both our experiments and previously published observations, the wild-type Epe1 protein and Swi6^{HP1} directly interact with each other. Adding increasing amounts of Epe1 leads to a corresponding increase in the amount of protein bound to Swi6^{HP1}. This interaction was retained in the presence and absence of EDTA suggesting that divalent metals such as Fe (II) which can bind to the JmjC domain are not a pre-requisite for the interaction between these two proteins (**Figure 2A, lanes 1-3 and 7-9**). However, to our surprise, Epe1 H297A exhibits a complete loss of interaction with Swi6^{HP1} resembling our earlier co-immunoprecipitation and ChIP measurements (**Figure 2A, lanes 4-6 and 10-12**). Since our binding assays are performed in the absence of co-factors required for oxidative demethylation, these results demonstrate that the interaction between Epe1 and Swi6^{HP1} and its loss upon mutation of a co-factor binding residue is independent of any enzymatic activity.

To rule out the possibility that any potential post-translational modifications of Swi6^{HP1} in fission yeast does not alter the conclusions of our experiments, we purified 3X FLAG- Swi6^{HP1} directly from fission yeast cells and used this purified protein in our binding assays. Our *in vitro* binding assays qualitatively resemble experiments performed using recombinant 3X FLAG-Swi6^{HP1} obtained from *E.coli* (**Supplementary Figure 2B**). Hence, the regulation of the interaction between Epe1 and Swi6 is independent of any potential Swi6 post-translational modifications but critically dependent on co-factor binding residues that map to the JmjC domain.HP1 proteins bind to sites of H3K9 methylation via a conserved chromodomain (CD)

and then recruit proteins that are important for transcriptional gene silencing through a conserved chromoshadow (CSD) domain. We verified that the interaction between Epe1 and Swi6^{HP1} is sensitive to a point mutation (Swi6^{HP1} L315E) that disrupts Swi6^{HP1} CSD dependent protein interactions (Canzio et al., 2013) (**Figure 2B**). Hence, our binding assays recapitulate an important and conserved feature of how Swi6^{HP1} interacts with diverse chromatin associated factors. To narrow down the region of Epe1 that interacts with Swi6^{HP1}, we used an *in vitro* translation system with rabbit reticulocyte lysates to generate two Epe1 fragments: 1) An N terminal fragment that includes the JmjC domain (1-600 amino acids) and, 2) a C-terminal fragment with no assigned function. The N terminal fragment which includes the JmjC domain interacts with Swi6^{HP1} and this interaction is sensitive to mutations that affect co-factor binding (Epe1 H297A and Epe1 Y307A). The C-terminal fragment fails to show any significant degree of interaction (**Supplementary figure 2C**). In addition, we compared the stabilities of the wild-type and mutant proteins using isothermal calorimetry measurements (**Supplementary Figure 2D**). Wild-type Epe1 and Epe1 H297A exhibit similar denaturation temperatures implying that the H297A point mutation does not destabilize the protein or lead to gross alterations in protein structure.

Since Epe1 shares conserved residues with active histone demethylases, we tested for a potential role that co-factors might play in regulating the interaction between Epe1 and Swi6^{HP1}. We performed *in vitro* binding assays in the presence of cobalt and N-oxalyl glycine (NOG) which are structural analogs of iron and α-ketoglutarate. Since cobalt and NOG cannot participate in oxidative demethylation, our binding reactions uniquely test for non-enzymatic functions associated with co-factor binding. The addition of cobalt and NOG leads to an increase in the interaction between Epe1 and Swi6^{HP1} compared to binding assays performed in the absence of co-factors (**Figure 2C, lanes 1-3 and lanes 7-9 and 2D**). In addition, we also observe a modest increase in the case of the Epe1 H297A mutant which does not appear change in an Epe1 H297A concentration dependent manner (**Figure 2C, lanes 4-6 and lanes 10-12 and 2D**). Based on these results, we concluded that the “active” co-factor bound state of Epe1 but not enzymatic activity itself leads to increased Swi6^{HP1} binding. In contrast, *in vitro* binding assays performed using iron and α-ketoglutarate resemble binding assays carried out in the absence of co-factors (**Supplementary Figure 2E**). Given that our reactions are carried out under aerobic conditions, the oxidation of iron or the reduction of α–ketoglutarate during the time course of our *in vitro* binding assays could lead to its rapid dissociation from the JmjC domain.

H3K9 methylation stimulates complex formation between Epe1 and Swi6^{HP1}

Epe1 co-localizes with Swi6^{HP1} at sites of heterochromatin formation (Ayoub et al., 2003). Given that the two proteins directly interact with each other in solution, we considered whether these interactions are sufficient to direct Epe1 to sites of heterochromatin formation. This was important considering that Swi6^{HP1} is a highly dynamic heterochromatin associated factor that interacts with sites of H3K9 methylation on the millisecond to second timescale (Cheutin et al., 2004; Cheutin et al., 2003). One possibility is that Epe1 interacts with and accompanies Swi6^{HP1} during these transits between heterochromatin bound and unbound states. To test this model, we measured the interaction between Epe1 and Swi6^{HP1} in cells that completely lack H3K9 methylation. This can be achieved either by deleting the H3K9 methyltransferase, Clr4^{Suv39h} or replacing individual histone H3 copies with an H3K9R mutant allele. Compared to wild-type cells where Epe1 co-immunoprecipitates with Swi6^{HP1}, the loss of H3K9 methylation completely disrupts a direct biochemical interaction between the two proteins (**Figure 3A**). These results suggest that in cells, Epe1 and Swi6^{HP1} form a complex only in a heterochromatin specific context.

This loss of complex formation between Epe1 and Swi6^{HP1} was generalizable to other heterochromatin deficient mutants. Deleting histone deacetylases, Clr3 and Sir2 also causes a reduction in H3K9 methylation levels and Swi6^{HP1} occupancy at sites of heterochromatin formation (Alper et al., 2013; Buscaino et al., 2013; Yamada et al., 2005). We found that deleting either Clr3 or Sir2 also leads to a significant loss of interaction between Epe1 and Swi6^{HP1} similar to the loss of interaction we observed upon deleting Clr4^{Suv39h} (**Figure 3B**). These results suggest that H3K9 methylation and functional heterochromatin are pre-requisites for the formation of a complex between Epe1 and Swi6^{HP1} in cells. On the other hand, the deletion of a histone acetyltransferase, Mst2 which enhances heterochromatin assembly, did not alter the extent of the interaction between Epe1 and Swi6^{HP1} (**Supplementary Figure 3A**) (Reddy et al., 2011).

To interrogate whether this heterochromatin dependency has a biochemical basis, we reconstituted the requirement for H3K9 methylation in our *in vitro* binding assays. Similar to the experiments previously described, we used a fixed concentration of recombinant Swi6^{HP1} on beads and immunoprecipitated increasing amounts of Epe1. We performed these experiments in the presence of an unmodified N terminal H3 peptide (1-21 amino acids) or an H3K9 tri-methylated peptide of the same length. The interaction between Epe1 and Swi6^{HP1} remains unaltered in the presence of an unmodified H3 tail peptide (**Figure 3C, lanes 1-3 and lanes 7-9, 3D**). However, the addition of an H3K9me3 peptide leads to a significant increase in interaction between Epe1 and Swi6^{HP1} (**Figure 3C, lanes 13-15 and 3D**).

We reasoned that either Swi6^{HP1} or Epe1 could bind a modified H3K9me3 peptide leading to a conformational change that enhances their mutual affinity. Given the similarities that Epe1 shares with other active histone demethylases, the only known histone modification binding domain would be the JmjC domain. We used streptavidin pull down measurements comparing methylated and unmethylated histone H3 peptides (1-21 amino acids) and confirmed that Epe1 does indeed harbor a latent, previously undiscovered capacity to recognize an H3K9me3 peptide (**Supplementary Figure 3B and 3C**). In the case of Swi6^{HP1}, a conserved chromodomain (CD) participates in binding to H3K9 methylated histone tails (Jacobs et al., 2001). We purified a recombinant version of Swi6^{HP1} that has a tryptophan to alanine substitution within the chromodomain (Swi6^{HP1} W104A). This point mutation eliminates the capacity of Swi6^{HP1} to bind to H3K9 methylation (Canzio et al., 2013). We performed *in vitro* binding reactions comparing the interaction between Epe1 and a Swi6^{HP1} CD mutant (Swi6^{HP1} W104A) versus wild-type Swi6^{HP1}. Epe1 does not discriminate between wild-type Swi6^{HP1} or the Swi6^{HP1} CD mutant and interacts with both proteins to a similar extent (**Figure 3E**). These results are consistent with our earlier observations that the Swi6^{HP1} CSD is the primary site of interaction between Epe1 and Swi6^{HP1} (**Figure 2B**). Most notably, the addition of an H3K9me3 peptide leads to an increase in the interaction between Epe1 and the Swi6^{HP1} CD mutant which parallels our observations with wild-type Swi6^{HP1} (**Figure 3E**). Hence, our results suggest that H3K9me3 binding induces a conformational change in Epe1 that leads to a high-affinity state of interaction with Swi6^{HP1}.

Discovering the latent capacity of Epe1 to recognize H3K9me3 histone tails and its interactions with Swi6^{HP1} prompted us to ask whether Epe1 could function as a histone demethylase. Epe1 in isolation or in complex with a one to five molar ratio of Swi6^{HP1} does not demethylate H3K9me3 peptides. Under the same conditions JMJD2A catalyzes a 15 Da shift in peptide molecular weight corresponding to the removal of a single methyl group. (**Supplementary Figure 3D).** Our results are consistent with the prevailing notion that Epe1 lacks H3K9 demethylase activity and we extend these observations to demonstrate the Swi6^{HP1}-Epe1 complex does not lead to further activation of its putative enzymatic functions.

The non-enzymatic function of Epe1 is necessary and sufficient to disrupt epigenetic inheritance

We hypothesized that the primary function of Epe1 might be to disrupt heterochromatin assembly through its ability to inhibit Swi6^{HP1} in a heterochromatin specific context. The histone deacetylase, Clr3 and Epe1 have opposing functions in regulating nucleosome turnover and hence we considered the possibility that simply attenuating Clr3 recruitment is sufficient to disrupt epigenetic inheritance. The heterochromatin specific recruitment of Clr3 involves interactions with two distinct fission yeast HP1 proteins, Swi6^{HP1} and Chp2^{HP1} (Isaac et al., 2017; Motamedi et al., 2008; Sadaie et al., 2008; Yamada et al., 2005). We co-immunoprecipitated Clr3 and measured its interaction with Swi6^{HP1} in cells with a wild-type allele of Epe1 versus an Epe1 H297A mutant. We observed a significant increase in the interaction between Clr3 and Swi6^{HP1} in an Epe1 mutant background where Epe1 fails to interact with Swi6^{HP1} (**Figure 4A**). Hence, our results demonstrate a trade-off in biochemical interactions where Clr3 can switch places with Epe1. This positive change in the interaction between Clr3 and Swi6^{HP1} occurs in the absence of any increase in Swi6^{HP1} occupancy at sites of heterochromatin formation at the pericentromeric repeats (**Figure 4B**).

If the primary mechanism of Epe1 function is non-enzymatic and its role is to displace Clr3 from sites of heterochromatin formation, we predicted that artificially recruiting Clr3 to an ectopic site should subvert the anti-silencing functions of Epe1. To test this hypothesis, we engineered synthetic heterochromatin domains where *10X Tet operator (10XTetO)* and *10X Gal4 DNA binding sites (10X Gal4)* are placed upstream of an *ade6+* reporter gene. This enables us to initiate heterochromatin formation via TetR-Clr4-I recruitment and follow heterochromatin maintenance in the presence of an orthogonal heterochromatin effector that is recruited to the same locus via a Gal4 DNA binding domain (**Figure 4C**). In the absence of any additional chromatin modifiers, TetR-Clr4-I recruitment to this ectopic site (*10X Gal4-10X TetO-ade6+*) leads to the appearance of red colonies on –tetracycline containing medium. Upon addition of tetracycline, cells rapidly turn white consistent with a causal role for Epe1 in disrupting the sequence-independent inheritance of heterochromatin (**Figure 1C**). We fused the Gal4 DNA binding domain (Gal4 DBD) to two histone deacetylases, Clr3 (a class II histone deacetylase) and Sir2 (an NAD-dependent histone deacetylase) enabling these proteins to be constitutively tethered to the Gal4 DNA binding sequences. The TetR-Clr4-I fusion initiates heterochromatin formation and cells turn red on medium lacking tetracycline with or without Gal4-Clr3 and Gal4-Sir2 (**Figure 4D**). However, upon exposure to tetracycline, the constitutive tethering of Clr3 but not Sir2 promotes stable maintenance. Cells exhibit a red and sectored phenotype despite Epe1 still being present in these cells (**Figure 4D**). These phenotypes are remarkably similar to cells that lack Epe1 (*epe1Δ*). The phenotypic changes also correlate with changes in H3K9 methylation levels associated with the *ade6+* reporter gene which we measured using ChIP-qPCR (**Figure 4E, F**). Cells maintain high H3K9me2 levels in the presence of Gal4-Clr3 after tetracycline addition similar to phenotypes we observe upon deleting Epe1 **(Figure 1C-E**). These results suggest that constitutively recruiting Clr3 to sites of heterochromatin formation bypasses the anti-silencing functions of Epe1 enabling heterochromatin maintenance.

Gal4-Clr3 does not initiate heterochromatin establishment *de novo* (**Supplementary figure 4A)**. Upon tethering Gal4-Clr3 in the absence of TetR-Clr4-I, cells remain white in the presence or absence of tetracycline and exhibit no H3K9me2 at the ectopic site (**Supplementary Figure 4B and 4C**). This lack of *de novo* silencing is consistent with the notion that HDAC proteins in fission yeast must collaborate with H3K9 methyltransferases to establish silent epigenetic states. Furthermore, simply expressing Clr3 without the artificial Gal4 DBD fusion causes cells to turn white on media containing +tetracycline (**Supplementary Figure**

4A). H3K9me2 levels are fully reset upon exposure to tetracycline demonstrating that it is the sequence-specific recruitment of Clr3 and not protein dosage which is the primary determinant of heterochromatin maintenance (**Supplementary Figure 4B**). Hence, Clr3 recruitment acts in *cis* to maintain silent epigenetic states and antagonize Epe1 activity. This property of heterochromatin maintenance is RNAi independent since cells continue to exhibit a red or sectored appearance in a Dicer deficient background (*dcr1Δ*) (**Supplementary Figure 4D**).

The read-write activity of Clr4^{Suv39h} is essential for the maintenance of silent epigenetic states in an *epe1Δ* background (Audergon et al., 2015; Ragunathan et al., 2015). The Clr4^{Suv39h} chromodomain mutant lacks the capacity to participate in a positive feedback loop where the protein binds to the product of its own enzymatic activity to propagate H3K9 methylation (Zhang et al., 2008). We replaced the wild-type allele of Clr4^{Suv39} with a mutant allele that lacks the chromodomain. Cells are initially red in –tetracycline medium but the deletion of the chromodomain results in cells that turn white on +tetracycline medium despite Clr3 being constitutively recruited (**Supplementary Figure 4E**). The H3K9me2 levels in *clr4ΔCD* strains are similar to that of wild-type cells during heterochromatin establishment but these mutant cells lack the capacity to epigenetically propagate H3K9 methylation during maintenance (**Supplementary Figure 4F-G**). Hence, the constitutive recruitment of Clr3 creates a chromatin environment that promotes the read-write activity of Clr4^{Suv39h} allowing epigenetic states to be propagated through an H3K9 methylation dependent positive feedback loop.

DISCUSSION

Our work demonstrates how Epe1, a fission yeast protein that belongs to the conserved JmjC family of enzymes, utilizes a unique, non-enzymatic mechanism to regulate heterochromatin assembly and epigenetic inheritance. A distinctive feature of the mechanism we have identified is that mutations which map to the putative catalytic domain of Epe1 disrupt its interaction with Swi6^{HP1}. Our work demonstrates that this disruption in protein-protein interactions mediated by Epe1 is its primary mechanism of action in the context of epigenetic inheritance. Our observations expand the possible modes of regulation that stem from protein domains that were solely thought to function as enzymes. In particular, our findings are most reminiscent of pseudokinases which represent a subfamily of proteins that structurally resemble active kinases but lack any catalytic activity. In some instances, stabilizing the “active conformation” of pseudokinases through substrate binding is a pre-requisite for its non-enzymatic function (Jamieson et al., 2018). Epe1 binds co-factors and modified histone peptides both which alter its capacity to interact with Swi6^{HP1} thus leveraging molecular attributes that would have otherwise been thought to regulate its enzymatic activity. Most notably, H3K9 methylation binding is absolutely essential for complex formation in cells and we demonstrate how this histone modification stimulates the interaction between the two proteins *in vitro*. Our findings provide an important rationale for why Epe1 mutants that are defective in co-factor binding act as multi-copy suppressors of an *epe1Δ* phenotype (Trewick et al., 2007; Zofall and Grewal, 2006). Protein overexpression simply compensates for a low affinity state of interaction between Epe1 and Swi6^{HP1} in the case of co-factor binding mutants (Epe1 H297A and Epe1 K314A) which in turn inhibits downstream heterochromatin assembly.

Previously, the deletion of Epe1 was thought to be the only context in which epigenetic states could be propagated in the absence of continuous heterochromatin initiation (Audergon et al., 2015; Ragunathan et al., 2015). Tethering Clr3 at an ectopic site renders heterochromatin completely refractory to the anti-silencing functions of Epe1. Our observations are in part, similar to previous findings relating to the fission yeast mating type locus where DNA binding proteins, Atf1 and Pcr1 recruit Clr3 to maintain stable epigenetic states following an RNAi dependent initiation mechanism (Wang and Moazed, 2017; Yamada et al., 2005). Our studies fully recapitulate the unique requirement for the sequence dependent recruitment of HDAC

proteins or other chromatin modifiers to function in *cis* in order to support the inheritance of silent epigenetic states in the presence of anti-silencing factors such as Epe1.

A major question which emerges is whether replication dependent and replication independent nucleosome turnover mechanisms are sufficient to reset epigenetic states in the absence of continuous initiation. The deletion of Epe1 suppresses nucleosome turnover at sites of heterochromatin formation whereas the deletion of Clr3 enhances this process {Aygun, 2013 #13}. Our studies demonstrate that this antagonistic relationship between Clr3 and Epe1 proteins is the defining molecular event that regulates epigenetic inheritance. We favor the idea that histone deacetylases such as Clr3 simply provide a chromatin environment that alters the read-write activity of Clr4^{Suv39h}. Altering the read-write activities of histone modifying enzymes allows them up to compete with genome-wide nucleosome turnover processes that would other reset existing epigenetic states. Epe1 plays a central role in regulating this process by forming an inhibitory complex with Swi6^{HP1} in a heterochromatin specific context. Our data fully supports the idea that enzymatic erasure is dispensable for regulating the inheritance of transcriptionally silent chromatin states in fission yeast. Although our minimalist representation of heterochromatin at an ectopic locus captures a unique requirement for Clr3, it is likely that Epe1 also displaces or interacts with other chromatin associated factors. A detailed proteomic analysis will be required to uncover changes in the Swi6^{HP1} interaction landscape upon deleting Epe1. For example, Epe1 directly interacts with members of the SAGA complex which leads to an increase in histone acetylation and stimulates transcription within heterochromatin repeats (Bao et al., 2019). In essence, our studies and others collectively suggest that a broad spectrum of non-enzymatic functions involving Epe1 may be both necessary and sufficient for regulating heterochromatin establishment, spreading and inheritance.

The question of whether Epe1 harbors any enzymatic properties remains controversial. Our experiments demonstrate that Epe1 binds to H3K9me3 peptides but this binding event does not translate to enzymatic activity. Previous studies demonstrate how HP1 proteins can potentially stimulate H3K36 demethylase activity of the *Drosophila* protein, dKDM4A (Lin et al., 2008). In the case of Epe1, we are unable to observe any demethylase activity in the presence or absence of Swi6. These results, by no means exclude the possibility that Epe1 may have enzymatic functions. We favor a model where different proteins that interact with Epe1 could act as positive or negative allosteric regulators which influence heterochromatin assembly to varying degrees. For example, Bdf2, a BRD4 homolog that localizes to heterochromatin boundaries along with Epe1, represents a possible candidate given that H3K9 methylation levels are negligible at the heterochromatin-euchromatin interface (Wang et al., 2013). It is also noteworthy that a histone demethylase like protein in *Neurospora,* DMM-1 shares many similarities with Epe1 and additionally lacks any *in vitro* enzymatic activity (Honda et al., 2010). DMM-1 also interacts with the HP1 homolog in *Neurospora* leading us to speculate that this surprising mode of heterochromatin regulation we uncovered in the case of Epe1 might also extend to other model systems.

We propose a *two-factor authentication model* for how Epe1 mediates its anti-silencing function in cells (**Figure 4G**). Epe1 localizes to sites of heterochromatin formation via two distinct but overlapping signals, namely co-factor binding and H3K9 methylation. Disrupting co-factor or H3K9 methylation binding leads to a concomitant reduction in the interaction between Epe1 and Swi6^{HP1}. Hence, H3K9 methylation in fission yeast cells provides a distinct context or chromatin environment that enables the formation of an inhibitory complex between Epe1 and Swi6^{HP1}. This remarkable biochemical property of Epe1 might enable the protein to only selectively interact with heterochromatin bound Swi6^{HP1} molecules as opposed to freely diffusing Swi6^{HP1} proteins. This distinction is important since Swi6^{HP1} is a highly dynamic molecule that resides at sites of heterochromatin formation on timescales ranging from a few milliseconds to

several seconds (Cheutin et al., 2004; Cheutin et al., 2003). This mechanism of chromatin context dependent binding might explain how Epe1 exerts a potent role during heterochromatin assembly and maintenance despite being expressed at levels that are twenty fold lower compared to Swi6^{HP1} (data not shown).

Our observations add to a growing list of proteins that resemble histone modifiers but have non-enzymatic functions during the establishment and maintenance of epigenetic states. In particular, JARID2, a subunit of the PRC2 complex that resembles JmjC domain containing proteins, plays a structural role in regulating PRC2 complex assembly (Kasinath et al., 2018; Son et al., 2013). The *Drosophila* protein dKDM4A, is another example of a histone demethylase that has non-enzymatic functions in the context of heterochromatin in flies (Colmenares et al., 2017). Two proteins involved in the *Arabidopsis* RNA dependent DNA methylation pathway, SUVH2 and SUVH9, resemble SET domain methyltransferases but lack enzymatic activity. Instead, both proteins recognize methylated DNA and are involved RNA pol V recruitment in plants (Johnson et al., 2008; Law et al., 2013).

Our studies provide a molecular framework for how a trade-off in the recruitment of distinct chromatin effectors can alter the stability and inheritance of silent epigenetic states (Grewal and Jia, 2007). Engineered epigenetic circuits based on the propagation of a non-native DNA modification reveal how the coordinated activities of synthetic read-write modules are sufficient to maintain epigenetic memory(Park et al., 2018). Our work provides an example of a natural system where histone modification dependent read-write mechanisms in the absence of enzymatic erasure sustain the inheritance of transcriptionally silent chromatin states. Epe1 employs an unusual mechanism where the putative catalytic domain regulates the stability of H3K9 methylation by tuning the read-write activity of Clr4^{Suv39h} which in fission yeast appears to be sensitive to the recruitment of HDAC proteins. The read-write activity of Clr4^{Suv39h} competes with passive replication dependent and independent turnover mechanisms. Altering nucleosome turnover rates creates epigenetic domains that remain stable and heritable across multiple generations. Our results outline a molecular logic as to how the putative catalytic domain of Epe1 alters heterochromatin specific interactions and broadens the spectrum of regulatory pathways that control the assembly and inheritance of silent epigenetic states.

ACKNOWLEDGEMENTS

We thank Ryan Baldridge, Patrick O'Brien and the Chromatin Club at the University of Michigan for creating a supportive environment, insightful suggestions and critical feedback. We thank Hiten Madhani, Danesh Moazed and Songtao Jia for yeast strains. We also thank Danesh Moazed for sharing the Swi6 primary antibody which has been used for all of co-immunoprecipitation and ChIP experiments. We than Nahid Iglesias for kindly sharing co-immunoprecipitation protocols that preserve heterochromatin bound complexes. This work was supported by startup funds from the Regents of the University of Michigan.

MATERIALS AND METHODS

Plasmids

Plasmids containing Epe1 wild-type and point mutants were constructed by modified existing pFA6a C-terminal tagging plasmids. Point mutations were introduced by designing primers using guidelines described in Quick Change mutagenesis protocols. A ligation independent cloning approach was used to construct pFastBac vectors containing wild-type Epe1 and Epe1 H297A mutant for recombinant protein expression. 3X FLAG Swi6 was cloned into existing pGEX vectors downstream of the prescission protease cleavage site using Gibson assembly. The construction of the 10X gal4-10X tetO-ade6 plasmid involved modifying plasmids containing a 10X tetO sequence and sub-cloning Gal4 UAS sequences derived from a

Drosophila pVALIUM 10X UAS vector. Vectors containing Gal4-Clr3 or Gal4-Sir2 were made using a modified pDual vector with an nmt1 promoter that enables facile incorporation of genetic payloads at the leu1 locus in fission yeast {Matsuyama, 2004 #138}. Further details regarding plasmid construction are readily available upon request.

Strains

All strains were constructed using a PCR-based gene targeting approach {Bahler, 1998 #139}. In cases where we generated point mutations of Epe1, we reintroduced the full length wild-type or mutant gene in *epe1Δ* strains. All strains were genotyped using colony PCR assays. We subsequently verified protein expression using western blots for each of the mutant strains. Strains with 10X gal4-10X tetO-ade6 were constructed using an FOA based selection strategy based on disrupting the endogenous *ura4* locus. Strains with Gal4-Clr3 or Gal4-Sir2 were made by digesting pDual vectors with a Not1 restriction enzyme followed by transformations and –LEU based selection. Other deletions of heterochromatin associated factors was achieved either by PCR-based gene targeting approaches or by a cross followed by random spore analysis and PCR based screening to select for colonies that harbored the reporter gene, All strains used in this study are listed in Table S1. Further details regarding strain construction are readily available upon request.

Cell lysis, Co-immunoprecipitation and Western blotting

1.5 L of fission yeast cells cells were grown in YEA medium at 32℃ to an OD_{600} =3.5 and harvested by centrifugation. The cell pellets were washed with 10 ml TBS pH 7.5, re-suspended in 1.5 ml lysis buffer (30 mM Hepes pH 7.5, 100 mM NaCl, 0.25% Triton X-100, 5 mM $MgCl_2$, 1 mM DTT) and cell suspension was snap-frozen into liquid nitrogen to form yeast “balls” and cryogenically ground using a SPEX 6875D Freezer/Mill. The frozen cell powder was thawed at room temperature and re-suspended in an additional 10 ml of lysis buffer with protease inhibitor cocktail and 1 mM PMSF. The cell lysates were subjected to two rounds of centrifugation at 18000 rpm for 5 and 30 mins in a JA-25.50 rotor (Beckman). Bradford assay was used to normalize protein levels for co-immunoprecipitation and immunoblot analysis. Protein G Magnetic Beads were pre-incubated with antibody for 4 h and cross-linked with 10 volumes of cross-linking buffer containing 20 mM DMP (3 mg DMP/ml of 0.2 M Boric Acid pH 9) for 30 min at room temperature by rotating. Cross linking was quenched by washing twice and incubated with 0.2 M ethanolamine pH 8 for 2 h at room temperature by rotating. The cell lysates were then incubated with antibody cross-linked beads for 3 hrs at 4℃. Beads were washed 3 times in 1ml lysis buffer 5 mins each, then eluted with 500 μl of 10 mM ammonium hydroxide, the ammonium hydroxide was evaporated using speed vac (SPC-100H) for 5 h and re-suspended in SDS sample buffer. Samples were resolved on SDS-PAGE and transferred to PVDF membranes. Immunoblotting was performed by blocking PVDF membrane in Tris-buffered saline (TBS) pH 7.5 with 0.1% Tween-20 (TBST) containing 5% non-fat dry milk and subsequently probed with desired primary antibodies and secondary antibodies. Blots were developed by ECL method and detected with Bio-Rad ChemiDoc Imaging System.

Chromatin Immunoprecipitaion (ChIP)

Cells were grown till late log phase (OD 600- 1.3 to 1.8) in yeast extract supplemented with adenine (YEA) or YEA containing tetracycline (2.5μg/ml) medium and fixed with 1% formaldehyde for 15 min at room temperature (RT). 130 mM glycine was then added to quench the reaction and incubated for 5 min at RT. The cells were harvested by centrifugation, and

washed twice with TBS (50 mM Tris, pH 7.6, 500 mM NaCl). Cell pellets were resuspended in 300 μl lysis buffer (50 mM Hepes-KOH, pH 7.5, 100 mM NaCl, 1mM EDTA, 1% Triton X-100, 0.1% SDS, and protease inhibitors) to which 500 μL 0.5 mm glass beads were added and cell lysis was carried out by bead beating using Omni Bead Ruptor at 3000 rpm x 30sec x 10 cycles. Tubes were punctured and the flow-through was collected in a new tube by centrifugation which was subjected sonication to obtain the fragment sizes of roughly 100-500 bp long. After sonication the extract was centrifuged for 15 min at 13000 rpm at 4°C. The soluble chromatin was then transferred to a fresh tube and normalized for protein concentration by the Bradford assay. For each normalized sample, 25μL lysate was saved as input, to which 225 μL of 1xTE/1% SDS were added (TE: 50 mM Tris pH 8.0, 1 mM EDTA). Dynabeads Protein A were preincubated with Anti-H3K9me2 antibody (Abcam, ab1220). For each immunoprecipitation, 2 ug antibody coupled to 30μL beads was added to 400μL soluble chromatin, and the final volume of 500μL was achieved by adding lysis buffer. Samples were incubated for 2h at 4°C, the beads were collected on magnetic stands, and washed 3 times with 1 ml lysis buffer and once with 1 ml TE. For eluting bound chromatin, 100μL elution buffer I (50 mM Tris pH 8.0, 10mM EDTA, 1% SDS) was added and the samples were incubated at 65°C for 5 min. The eluate was collected and incubated with 150 μL 1xTE/0.67% SDS in the same way. Input and immunoprecipitated samples were finally incubated overnight at 65°C to reverse crosslink for more than 6 hours. 60μg glycogen, 100 μg proteinase K (Roche), 44 ul of 5M LiCl, and 250 ul of 1xTE was added to each sample and incubation was continued at 55°C for 1h. Phenol/chloroform extraction was carried out for all the samples followed by ethanol precipitation. Immuno-precipitated DNA was resuspended in 100μL of 10 mM Tris pH 7.5 and 50 mM NaCl and was used for qPCR (SYBR Green) using an Eppendorf Mastercycler Realplex. For extra crosslinking, prior to fixing with 1% formaldehyde, the cultures were incubated at 18°C for 2 hours in a shaking incubator. The cells were pelleted and resuspended in 4.5 ml of 1x PBS. To this 1.5mM EGS (Ethylene glycol bis[succinimidylsuccinate], Pierce (Fisher) was added and the samples were incubated at RT for 20 min with mild shaking before adding 1 % formaldehyde. The samples were then processed as mentioned above.

Protein purification

His-MBP-TEV cleavage site-Epe1 genes were cloned into pFastBac vector (Thermo Fisher Scientific) and used for Bacmid generation. Low-titer baculoviruses were produced by transfecting Bacmid into Sf21 cells using Cellfectin II reagent (Gibco). Full length S. pombe Epe1 protein (wild-type and mutant) were expressed in Hi5 cells infected by high titer baculovirus which were amplified from Sf21 cells. After 44 hrs of infection, Hi5 cells were harvested and lysed in buffer A (30 mM Tris-HCl (pH 8.0), 500 mM NaCl, 5 mM EDTA, 5 mM β-mercaptoethanol with protease inhibitor cocktails) using Emulsiflex-C3 (Avestin). The cleared cell lysate was applied to Amylose resin (New England Biolabs) followed by washing with buffer A and elution with buffer A containing 10 mM maltose. The N-terminal His-MBP tag can be removed by TEV protease cleavage which was used to evaluate protein solubility. Proteins were further purified using a Superdex 200 (GE Healthcare) size exclusion columns. The protein was concentrated up to in a storage buffer containing 30 mM Tris-HCl (pH 8.0), 500 mM NaCl, 30% Glycerol and 1 mM TCEP.

***In vitro* Binding Assay**

In vitro binding assays were performed by immobilizing recombinant 3X FLAG-Swi6 on 25 μl of FLAG M2 beads which were incubated with 3 different concentrations of recombinant

MBP-Epe1 or MBP-Epe1 H297A in 600 μl binding buffer containing 20 mM Hepes pH 7.5, 150 mM NaCl, 5 mM $MgCl_2$, 10% Glycerol, 0.25% Triton -X 100, 1 mM DTT. Reactions were incubated at 4 ºC for 2 hrs and washed 3 times in 1ml washing buffer (20 mM Hepes pH 7.5, 150 mM NaCl, 5 mM $MgCl_2$, 10% Glycerol, 0.25% Triton -X 100, 1 mM DTT) 5 min each, added 30μl SDS sample buffer followed by incubation at 95°C for 5 min. Proteins were separated through SDS-PAGE and transferred to PVDF membrane followed by incubation with anti-MBP monoclonal antibody (E8032S, NEB) and M2 Flag antibody (A8592, Sigma). Depending on the experiment, we added co-factors Cobalt chloride (100μM) and N-oxalylglycine (2mM) or iron sulfate (100μM) and α–ketoglutarate (1mM) or 5μg of H3 peptides (1-21 amino acids) that were either chemically modified (H3K9me3) or unmodified (H3K9me0). Western blot data for *in vitro* binding assays were analyzed using ImageJ software. First, band intensities for the Epe1 IP and Swi6 IP was measured by ImageJ and the Epe1 IP values were divided by Swi6 IP values. The highest value of Epe1 IP / Swi6 IP is normalized to 1 and all other values were measured relative to this.

Demethylase Assay

Mass spectrometry-based demethylase assays were performed using 5μg MBP-Epe1, 10μg Swi6, 20μM peptide (H3K9me3 peptide sequence used in this assay: NH_2-ARTKQTAR(K9me3)STGGKA-amide), 50 mM HEPES (pH 7.5), 50 mM NaCl, 100 μM Ammonium iron (II) sulfate hexahydrate, 1 mM L-ascorbic acid, 1 mM α-ketoglutarate. Reaction mixtures were incubated at 37°C for 3 hrs, quenched with an equal volume of 1% trifluoroacetic acid, and stored at - 20°C. In parallel, we also performed demethylase assays using equivalent amounts of purified JMJD2A (protein amounts equalized using SDS-PAGE gels). Samples were thawed and desalted using a ZipTip (Millipore). ZipTip was first equilibrated twice with wetting solution (50% Acetonitrile) and twice with equilibration solution (0.1% Trifluoroacetic acid) followed by 10μl samples bound to ZipTip and washed with washing solution (0.1% Trifluoroacetic acid) before elution with 4μl of 0.1% Trifluoroacetic acid/50% Acetonitrile. Matrix-assisted laser desorption ionization (MALDI) mass spectrometry was performed using a Waters Tofspec-2E in reflectron mode with delayed extraction (Department of Chemistry, University of Michigan).

***In vitro* translation assays**

To identify minimal Epe1 fragments that bind to Swi6 and to compare Swi6 binding affinity of Epe1 WT, H297A and Y307A, Epe1 mutant proteins were translated in *vitro* using TNT T7-coupled reticulocyte lysate (Promega) with ^{35}S-labeled methionine (Roche). *In vitro* translated target proteins were incubated with Flag-tagged Swi6 at 4 °C for 20 min. Flag beads (Please find the product information) pre-equilibrated with buffer B containing 30 mM Tris-HCl (pH 8.0), 50 mM NaCl, 1 mM DTT and 0.1% NP-40 (w/v) were mixed and incubated at 4 °C for 45 min with rotation. The beads were washed three times with buffer B, and bead-bound proteins were separated by SDS-PAGE. Dried gels were analyzed by overnight exposure of a phosphor imager plate.

Streptavidin pull down assay

Biotinylated peptides (50nM) either unmodified H3 or K9-trimethyl H3 (K9me3) were pre-incubated with streptavidin Dynabeads (Invitrogen) in binding buffer (30mM Tris-HCl [pH 7.5], 300mM NaCl, 0.1% Triton X-100, 5% Glycerol, 2.5% BSA) for 1 hr at 4°C. Peptide-bound beads were incubated with 3 different concentrations of recombinant Epe1 for 2 hrs at 4°C in binding

buffer. The beads were then washed 3 times with washing buffer (30mM Tris-HCl [pH 7.5], 300mM NaCl, 0.1% Triton X-100, 5% Glycerol, 2.5% BSA) and bound proteins were eluted by boiling the beads in SDS sample buffer. The input and bound proteins were resolved by SDS – polyacrylamide gel electrophoresis (SDS-PAGE) and analyzed by immunoblotting with MBP antibody (E8032S, NEB).

REFERENCES

Al-Sady, B., Madhani, H.D., and Narlikar, G.J. (2013). Division of labor between the chromodomains of HP1 and Suv39 methylase enables coordination of heterochromatin spread. Mol Cell *51*, 80-91.

Allis, C.D., and Jenuwein, T. (2016). The molecular hallmarks of epigenetic control. Nat Rev Genet *17*, 487-500.

Alper, B.J., Job, G., Yadav, R.K., Shanker, S., Lowe, B.R., and Partridge, J.F. (2013). Sir2 is required for Clr4 to initiate centromeric heterochromatin assembly in fission yeast. EMBO J *32*, 2321-2335.

Audergon, P.N., Catania, S., Kagansky, A., Tong, P., Shukla, M., Pidoux, A.L., and Allshire, R.C. (2015). Epigenetics. Restricted epigenetic inheritance of H3K9 methylation. Science *348*, 132-135.

Aygun, O., Mehta, S., and Grewal, S.I. (2013). HDAC-mediated suppression of histone turnover promotes epigenetic stability of heterochromatin. Nat Struct Mol Biol *20*, 547-554.

Ayoub, N., Noma, K., Isaac, S., Kahan, T., Grewal, S.I., and Cohen, A. (2003). A novel jmjC domain protein modulates heterochromatization in fission yeast. Mol Cell Biol *23*, 4356-4370.

Bao, K., Shan, C.M., Moresco, J., Yates, J., 3rd, and Jia, S. (2019). Anti-silencing factor Epe1 associates with SAGA to regulate transcription within heterochromatin. Genes Dev *33*, 116-126.

Bayne, E.H., White, S.A., Kagansky, A., Bijos, D.A., Sanchez-Pulido, L., Hoe, K.L., Kim, D.U., Park, H.O., Ponting, C.P., Rappsilber, J.*, et al.* (2010). Stc1: a critical link between RNAi and chromatin modification required for heterochromatin integrity. Cell *140*, 666-677.

Braun, S., Garcia, J.F., Rowley, M., Rougemaille, M., Shankar, S., and Madhani, H.D. (2011). The Cul4-Ddb1(Cdt)(2) ubiquitin ligase inhibits invasion of a boundary-associated antisilencing factor into heterochromatin. Cell *144*, 41-54.

Buscaino, A., Lejeune, E., Audergon, P., Hamilton, G., Pidoux, A., and Allshire, R.C. (2013). Distinct roles for Sir2 and RNAi in centromeric heterochromatin nucleation, spreading and maintenance. EMBO J *32*, 1250-1264.

Canzio, D., Liao, M., Naber, N., Pate, E., Larson, A., Wu, S., Marina, D.B., Garcia, J.F., Madhani, H.D., Cooke, R.*, et al.* (2013). A conformational switch in HP1 releases auto-inhibition to drive heterochromatin assembly. Nature *496*, 377-381.

Cheutin, T., Gorski, S.A., May, K.M., Singh, P.B., and Misteli, T. (2004). In vivo dynamics of Swi6 in yeast: evidence for a stochastic model of heterochromatin. Mol Cell Biol *24*, 3157-3167.

Cheutin, T., McNairn, A.J., Jenuwein, T., Gilbert, D.M., Singh, P.B., and Misteli, T. (2003). Maintenance of stable heterochromatin domains by dynamic HP1 binding. Science *299*, 721-725.

Chory, E.J., Calarco, J.P., Hathaway, N.A., Bell, O., Neel, D.S., and Crabtree, G.R. (2019). Nucleosome Turnover Regulates Histone Methylation Patterns over the Genome. Mol Cell *73*, 61-72 e63.

Coleman, R.T., and Struhl, G. (2017). Causal role for inheritance of H3K27me3 in maintaining the OFF state of a Drosophila HOX gene. Science *356*.

Colmenares, S.U., Swenson, J.M., Langley, S.A., Kennedy, C., Costes, S.V., and Karpen, G.H. (2017). Drosophila Histone Demethylase KDM4A Has Enzymatic and Non-enzymatic Roles in Controlling Heterochromatin Integrity. Dev Cell *42*, 156-169 e155.

Deal, R.B., Henikoff, J.G., and Henikoff, S. (2010). Genome-wide kinetics of nucleosome turnover determined by metabolic labeling of histones. Science *328*, 1161-1164.
Fischer, T., Cui, B., Dhakshnamoorthy, J., Zhou, M., Rubin, C., Zofall, M., Veenstra, T.D., and Grewal, S.I. (2009). Diverse roles of HP1 proteins in heterochromatin assembly and functions in fission yeast. Proc Natl Acad Sci U S A *106*, 8998-9003.
Grewal, S.I., and Jia, S. (2007). Heterochromatin revisited. Nat Rev Genet *8*, 35-46.
Hall, I.M., Shankaranarayana, G.D., Noma, K., Ayoub, N., Cohen, A., and Grewal, S.I. (2002). Establishment and maintenance of a heterochromatin domain. Science *297*, 2232-2237.
Honda, S., Lewis, Z.A., Huarte, M., Cho, L.Y., David, L.L., Shi, Y., and Selker, E.U. (2010). The DMM complex prevents spreading of DNA methylation from transposons to nearby genes in Neurospora crassa. Genes Dev *24*, 443-454.
Horton, J.R., Upadhyay, A.K., Hashimoto, H., Zhang, X., and Cheng, X. (2011). Structural basis for human PHF2 Jumonji domain interaction with metal ions. J Mol Biol *406*, 1-8.
Iglesias, N., Currie, M.A., Jih, G., Paulo, J.A., Siuti, N., Kalocsay, M., Gygi, S.P., and Moazed, D. (2018). Automethylation-induced conformational switch in Clr4 (Suv39h) maintains epigenetic stability. Nature.
Isaac, R.S., Sanulli, S., Tibble, R., Hornsby, M., Ravalin, M., Craik, C.S., Gross, J.D., and Narlikar, G.J. (2017). Biochemical Basis for Distinct Roles of the Heterochromatin Proteins Swi6 and Chp2. J Mol Biol *429*, 3666-3677.
Iwase, S., Lan, F., Bayliss, P., de la Torre-Ubieta, L., Huarte, M., Qi, H.H., Whetstine, J.R., Bonni, A., Roberts, T.M., and Shi, Y. (2007). The X-linked mental retardation gene SMCX/JARID1C defines a family of histone H3 lysine 4 demethylases. Cell *128*, 1077-1088.
Jacobs, S.A., Taverna, S.D., Zhang, Y., Briggs, S.D., Li, J., Eissenberg, J.C., Allis, C.D., and Khorasanizadeh, S. (2001). Specificity of the HP1 chromo domain for the methylated N-terminus of histone H3. EMBO J *20*, 5232-5241.
Jamieson, S.A., Ruan, Z., Burgess, A.E., Curry, J.R., McMillan, H.D., Brewster, J.L., Dunbier, A.K., Axtman, A.D., Kannan, N., and Mace, P.D. (2018). Substrate binding allosterically relieves autoinhibition of the pseudokinase TRIB1. Sci Signal *11*.
Johnson, L.M., Law, J.A., Khattar, A., Henderson, I.R., and Jacobsen, S.E. (2008). SRA-domain proteins required for DRM2-mediated de novo DNA methylation. PLoS genetics *4*, e1000280.
Kasinath, V., Faini, M., Poepsel, S., Reif, D., Feng, X.A., Stjepanovic, G., Aebersold, R., and Nogales, E. (2018). Structures of human PRC2 with its cofactors AEBP2 and JARID2. Science *359*, 940-944.
Laprell, F., Finkl, K., and Muller, J. (2017). Propagation of Polycomb-repressed chromatin requires sequence-specific recruitment to DNA. Science *356*, 85-88.
Law, J.A., Du, J., Hale, C.J., Feng, S., Krajewski, K., Palanca, A.M., Strahl, B.D., Patel, D.J., and Jacobsen, S.E. (2013). Polymerase IV occupancy at RNA-directed DNA methylation sites requires SHH1. Nature *498*, 385-389.
Lin, C.H., Li, B., Swanson, S., Zhang, Y., Florens, L., Washburn, M.P., Abmayr, S.M., and Workman, J.L. (2008). Heterochromatin protein 1a stimulates histone H3 lysine 36 demethylation by the Drosophila KDM4A demethylase. Mol Cell *32*, 696-706.
Moazed, D. (2011). Mechanisms for the inheritance of chromatin states. Cell *146*, 510-518.
Motamedi, M.R., Hong, E.J., Li, X., Gerber, S., Denison, C., Gygi, S., and Moazed, D. (2008). HP1 proteins form distinct complexes and mediate heterochromatic gene silencing by nonoverlapping mechanisms. Mol Cell *32*, 778-790.
Nicetto, D., Donahue, G., Jain, T., Peng, T., Sidoli, S., Sheng, L., Montavon, T., Becker, J.S., Grindheim, J.M., Blahnik, K.*, et al.* (2019). H3K9me3-heterochromatin loss at protein-coding genes enables developmental lineage specification. Science *363*, 294-297.
Park, M., Patel, N., Keung, A.J., and Khalil, A.S. (2018). Engineering Epigenetic Regulation Using Synthetic Read-Write Modules. Cell.

Ragunathan, K., Jih, G., and Moazed, D. (2015). Epigenetics. Epigenetic inheritance uncoupled from sequence-specific recruitment. Science *348*, 1258699.
Reddy, B.D., Wang, Y., Niu, L., Higuchi, E.C., Marguerat, S.B., Bahler, J., Smith, G.R., and Jia, S. (2011). Elimination of a specific histone H3K14 acetyltransferase complex bypasses the RNAi pathway to regulate pericentric heterochromatin functions. Genes Dev *25*, 214-219.
Sadaie, M., Kawaguchi, R., Ohtani, Y., Arisaka, F., Tanaka, K., Shirahige, K., and Nakayama, J. (2008). Balance between distinct HP1 family proteins controls heterochromatin assembly in fission yeast. Mol Cell Biol *28*, 6973-6988.
Shimada, A., Dohke, K., Sadaie, M., Shinmyozu, K., Nakayama, J., Urano, T., and Murakami, Y. (2009). Phosphorylation of Swi6/HP1 regulates transcriptional gene silencing at heterochromatin. Genes Dev *23*, 18-23.
Son, J., Shen, S.S., Margueron, R., and Reinberg, D. (2013). Nucleosome-binding activities within JARID2 and EZH1 regulate the function of PRC2 on chromatin. Genes Dev *27*, 2663-2677.
Trewick, S.C., Minc, E., Antonelli, R., Urano, T., and Allshire, R.C. (2007). The JmjC domain protein Epe1 prevents unregulated assembly and disassembly of heterochromatin. EMBO J *26*, 4670-4682.
Tsukada, Y., Fang, J., Erdjument-Bromage, H., Warren, M.E., Borchers, C.H., Tempst, P., and Zhang, Y. (2006). Histone demethylation by a family of JmjC domain-containing proteins. Nature *439*, 811-816.
Verdel, A., Jia, S., Gerber, S., Sugiyama, T., Gygi, S., Grewal, S.I., and Moazed, D. (2004). RNAi-mediated targeting of heterochromatin by the RITS complex. Science *303*, 672-676.
Volpe, T.A., Kidner, C., Hall, I.M., Teng, G., Grewal, S.I., and Martienssen, R.A. (2002). Regulation of heterochromatic silencing and histone H3 lysine-9 methylation by RNAi. Science *297*, 1833-1837.
Wang, J., Reddy, B.D., and Jia, S. (2015). Rapid epigenetic adaptation to uncontrolled heterochromatin spreading. eLife *4*.
Wang, J., Tadeo, X., Hou, H., Tu, P.G., Thompson, J., Yates, J.R., 3rd, and Jia, S. (2013). Epe1 recruits BET family bromodomain protein Bdf2 to establish heterochromatin boundaries. Genes Dev *27*, 1886-1902.
Wang, X., and Moazed, D. (2017). DNA sequence-dependent epigenetic inheritance of gene silencing and histone H3K9 methylation. Science *356*, 88-91.
Whetstine, J.R., Nottke, A., Lan, F., Huarte, M., Smolikov, S., Chen, Z., Spooner, E., Li, E., Zhang, G., Colaiacovo, M.*, et al.* (2006). Reversal of histone lysine trimethylation by the JMJD2 family of histone demethylases. Cell *125*, 467-481.
Yamada, T., Fischle, W., Sugiyama, T., Allis, C.D., and Grewal, S.I. (2005). The nucleation and maintenance of heterochromatin by a histone deacetylase in fission yeast. Mol Cell *20*, 173-185.
Zhang, K., Mosch, K., Fischle, W., and Grewal, S.I. (2008). Roles of the Clr4 methyltransferase complex in nucleation, spreading and maintenance of heterochromatin. Nat Struct Mol Biol *15*, 381-388.
Zofall, M., and Grewal, S.I. (2006). Swi6/HP1 recruits a JmjC domain protein to facilitate transcription of heterochromatic repeats. Mol Cell *22*, 681-692.
Zofall, M., Yamanaka, S., Reyes-Turcu, F.E., Zhang, K., Rubin, C., and Grewal, S.I. (2012). RNA elimination machinery targeting meiotic mRNAs promotes facultative heterochromatin formation. Science *335*, 96-100.

Supplemental Table S1. Strains used in this study

Strains	Strains description	Strain sources	Figures strains used
KR18	*h⁻ leu1-32 ade6 M210 ura4Δ::10XTetO-ade6⁺ clr4⁺, trp1:natMX6-clr4p-TetR-clr4ΔCD*	Moazed lab	Figure 1 C, D, E
KR33	*h⁻ leu1-32 ade6? ura4Δ::10XTetO- ade6⁺ clr4⁺, trp1:natMX6-clr4p-TetR-clr4ΔCD, epe1Δ::kanMX6*	Moazed lab	Figure 1 C, D, E
KR283	*h⁻ leu1-32 ade6 M210 ura4Δ::10XTetO-ade6⁺ clr4⁺, trp1:natMX6-clr4p-TetR-clr4ΔCD, 3XFLAG-epe1-hphMX6*	This study	Figure 1 C, D, E
KR303	*h⁻ leu1-32 ade6 M210 ura4Δ::10XTetO -ade6⁺ clr4⁺, trp1:natMX6-clr4p-TetR-clr4ΔCD, 3XFLAG-epe1 H297A -hphMX6*	This study	Figure 1 C, D, E
KR844	*h⁻ leu1-32 ade6 M210 ura4Δ::10XTetO -ade6⁺ clr4+, trp1:natMX6-clr4p-TetR-clr4ΔCD, 3XFLAG-epe1 Y307A -hphMX6*	This study	Figure 1 C, D, E
KR846	*h⁻ leu1-32 ade6 M210 ura4Δ::10XTetO -ade6⁺ clr4⁺, trp1:natMX6-clr4p-TetR-clr4ΔCD, 3XFLAG-epe1 Y370A-hphMX6*	This study	Figure 1 C, D, E
KR840	*h⁻ leu1-32 ade6 M210 ura4Δ::10XTetO -ade6⁺ clr4⁺, trp1:natMX6-clr4p-TetR-clr4ΔCD, 3XFLAG-epe1 Y370F-hphMX6*	This study	Figure 1 C, D, E
KR24	*h⁻ leu1-32 ade6 M210 ura4Δ::10XTetO-ade6⁺, clr4Δ::kanMX6*	Moazed lab	Figure 1 C, D, E
KR342	*h⁺ leu1-32 otr1R(SphI)::ura4⁺ ura4-DS/E ade6 M210*	Moazed lab	Figure 1 E, G
KR471	*h⁻ leu1-32 epe1-3XFLAG- hphMX6*	Moazed lab	Figure 1 E, G
KR128	*h⁻ leu-32 epe1H297A-3XFLAG-hphMX6*	This study	Figure 1 E, G
KR769	*h⁺ leu1-32 ura4D18 imr1R(NcoI)::ura4⁺ oriL ade6 M216 epe1 Y307A-3XFLAG-hphMX6*	This study	Figure 1 E, G
KR705	*h⁺ otr1R(SphI)::ura4⁺ ura4-DS/E leu1-32 ade6 M210 epe1 Y370A -3XFLAG-hphMX6*	This study	Figure 1 E, G
KR205	*h⁻ leu-32 epe1 Y370F-3XFLAG-hphMX6*	This study	Figure 1 E, G
KR132	*h⁻ leu-32 epe1-3X-FLAG::hphMX6 swi6Δ::kanMX6*	Moazed lab	Figure 1 E, G
KR279	*h⁺ leu1-32 ura4D18 imr1R(NcoI)::ura4⁺ oriL ade6 M216 3XFLAG-epe1-hphMX6*	This study	Figure S1 C
KR285	*h⁺ leu1 – 32 ura4D18 imr1R(NcoI)::ura4⁺ oril ade6 M216 3XFLAG-epe1 H297A-hphMX6*	This study	Figure S1 C
KR228	*h⁺ otr1R(SphI)::ade6⁺ ura4Δ18 leu1-32 ade6 M210 H3.1/H3.2/H3.3 K9R epe13X-FLAG-hphMX6*	Moazed lab	Figure 3 A

KR130	*h⁻ leu-32 epe1 3X-FLAG-hphMX6 clr4Δ::kanMX6*	This study	Figure 3 A
KR724	*h⁻ leu-32 epe1 3X-FLAG hphMX6 clr3Δ::kanMX6*	This study	Figure 3 B
KR726	*h⁻ leu-32 epe1 H297A 3X-FLAG hphMX6 clr3Δ::kanMX6*	This study	Figure 3 B
KR728	*h⁻ leu-32 epe1 3X-FLAG-hphMX6 sir2Δ::kanMX6*	This study	Figure 3 B
KR730	*h⁻ leu-32 epe1 H297A 3X-FLAG-hphMX6 sir2Δ::kanMX6*	This study	Figure 3 B
KR732	*h⁻ leu1-32 ade6? ura4D18 mst2Δ::kanMX6 epe1 3X-FLAG-hphMX6*	This study	Figure S3 A
KR 734	*h⁻ leu1-32 ade6? ura4D18 mst2Δ::kanMX6 epe1 H297A 3X-FLAG-hphMX6*	This study	Figure S3 A
KR906	*h⁻ leu1-32 epe1 3X-FLAG hphMX6 clr3 3X-V5-natMX6*	This study	Figure 4 A
KR908	*h⁻ leu1-32 epe1 H297A-3XFLAG-hphMX6 clr3 3X-V5-natMX6*	This study	Figure 4 A
KR675	*h⁻ ade6 M210 ura4Δ::10XGal4-10XTetO-ade6⁺ natMX6-TetR-clr4-I, epe1⁺, leu1⁺:nmt1-gal4-sir2*	This study	Figure 4 D, E, F
KR677	*h⁻ ade6 M210 ura4Δ::10XGal-10XTetO-ade6⁺ natMX6-TetR-clr4-I epe1⁺, leu1⁺:nmt1-gal4-clr3*	This study	Figure 4 D, E, F
KR606	*h⁻ leu1-32 ade6 M210 ura4Δ::10XGal4-10XTetO-ade6⁺ trp1:natMX6-TetR-clr4-I*	This study	Figure 4 D, E, F
KR643	*h⁻ leu1-32 ade6 M210 10XTetO- ade6⁺ natMX6-TetR-Clr4-I, epe1Δ::kanMX6*	This study	Figure 4 D, E, F
KR1075	*h⁻ ade6 M210 ura4Δ::10XGal4-10XTetO-ade6⁺ trp1:natMX6-TetR-clr4-I leu1⁺:nmt1-gal4-clr3*	This study	Figure S4 A, B, C
KR1071	*h⁻ ade6 M210 ura4Δ::10XGal-10XTetO-ade6⁺ natMX6-TetR-clr4-I epe1⁺ leu1⁺:nmt1-clr3 (-gal4)*	This study	Figure S4 A, B, C
KR1067	*h⁻ ade6 M210 ura4Δ::10XGal-10XTetO- ade6⁺ natMX6-TetR-clr4-I epe1⁺ leu1⁺:nmt1-Gal4-clr3 hphMX6-NLS-clr4ΔCD*	This study	Figure S4 E, F, G
KR1103	*h⁻ ade6 M210 ura4Δ::10XGal4-10XTetO-ade6⁺ natMX6-TetR-clr4-I epe1⁺ leu1⁺:nmt1-gal4-clr3 dcr1Δ:: kanMX6*	This study	Figure S4 D

Figure 1

A

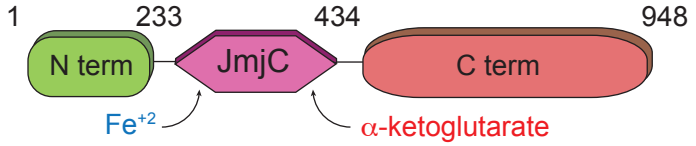


```
Sp Epe1  LMSAENSYTEFHIEFGGSSAYYNILDGCKIFYLI.........LVPSGWIYAVVTPCDTISIAGN
Ms PHF8  LMSVRDSYTDFHIDFGGTSVWYHVLKGEKIFYLI.........FIPTGWIHAVLTPVDCLAFGGN
Sc Jhd1  LMSVKDAYTDFHLDFAGTSVYYNVISGQKKFLLF.........MIPAGYIHAVYTPVDSLVFGGN
Hs KDM2A LMSVRGCYTDFHVDFGGTSVWYHIHQGGKVFWLI.........VIPSGWIHAVYTPTDTLVFGGN
```

B

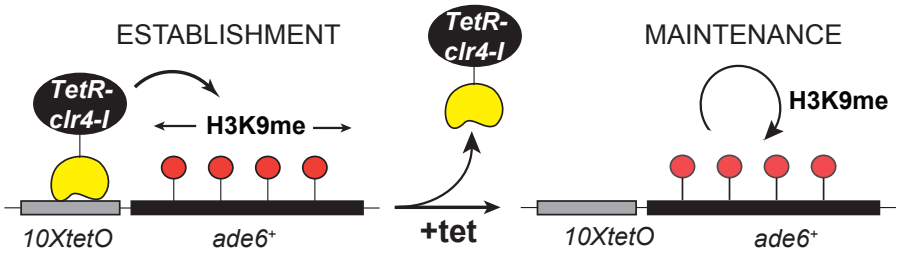

C

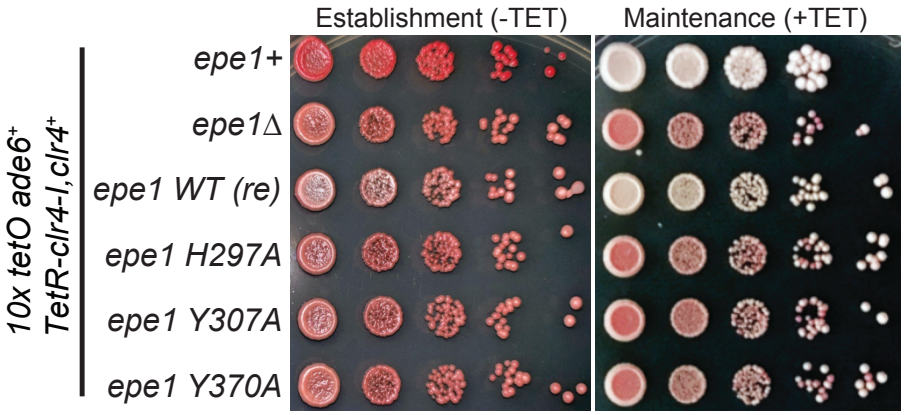

D

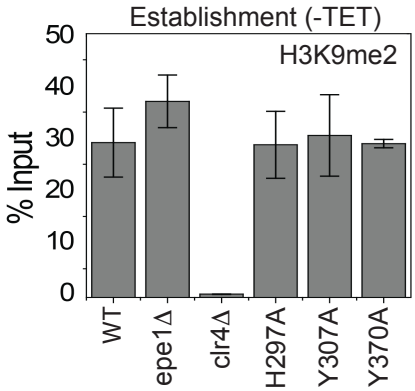

E

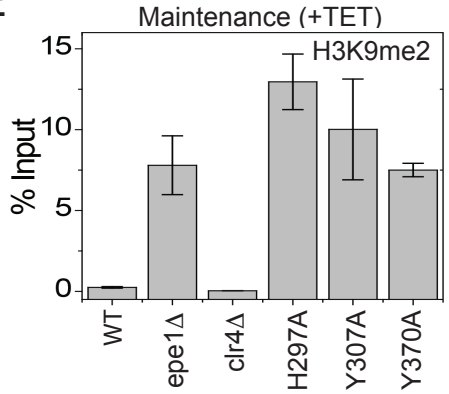

F

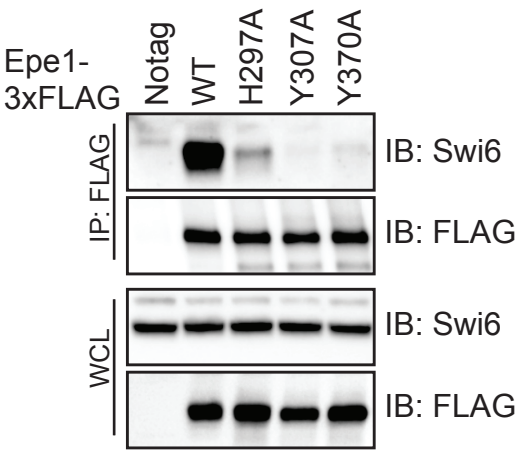

G

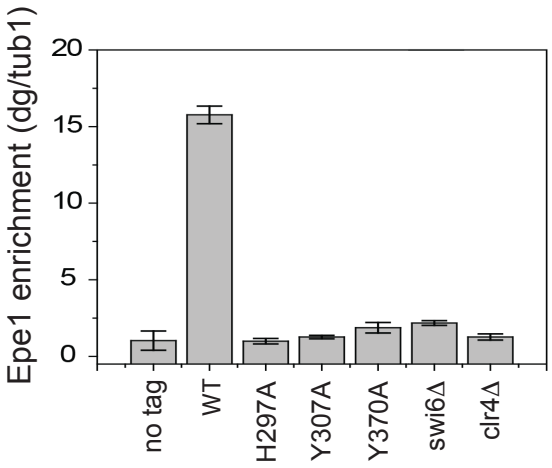

Figure 1: Mutations that affect co-factor binding disrupt the interaction between Epe1 and Swi6^{HP1}

A) Sequence alignment of related JmjC domain containing proteins reveals the identity of conserved residues in Epe1 that are involved in iron, Fe (II) and α-ketoglutarate binding. **B)** A reporter system to detect sequence-independent epigenetic inheritance. Heterochromatin initiation depends on TetR-Clr4-I binding (-tetracycline) leading to the establishment of H3K9 methylation at an ectopic site. The addition of tetracycline promotes TetR-Clr4-I dissociation to test for conditions where we can detect initiator independent maintenance of H3K9 methylation. **C)** A color based assay to detect the establishment and maintenance of epigenetic states. The establishment of epigenetic silencing (-tetracycline) leads to the appearance of red colonies. Epigenetic inheritance, indicated by red or sectored colonies, (+tetracycline) is critically dependent on Epe1 activity. **D)** ChIP-qPCR measurements of H3K9me2 levels at the ectopic site (*10X tetO ade6+*) during establishment (-tetracycline) in different Epe1 mutant strains (N=2). Error bars represent standard deviations. **E)** ChIP-qPCR measurements of H3K9me2 levels at the ectopic site (*10X tetO ade6+*) during maintenance (+tetracycline) in different Epe1 mutant strains (N=2). Error bars represent standard deviations. **F)** Western blots of co-immunoprecipitation measurements to test for an interaction between Epe1-3XFLAG and Swi6^{HP1}. The interaction is preserved in wild-type cells and is completely disrupted in Epe1 co-factor binding mutants. **G)** ChIP-qPCR measurements of Epe1 occupancy at endogenous sites of heterochromatin formation (*dg* pericentromeric repeats) (N=2). Error bars represent standard deviations. Epe1 enrichment is reduced to near background levels in the case of Epe1 co-factor binding mutants and their levels are similar to *swi6Δ* and *clr4Δ* cells.

Figure 2

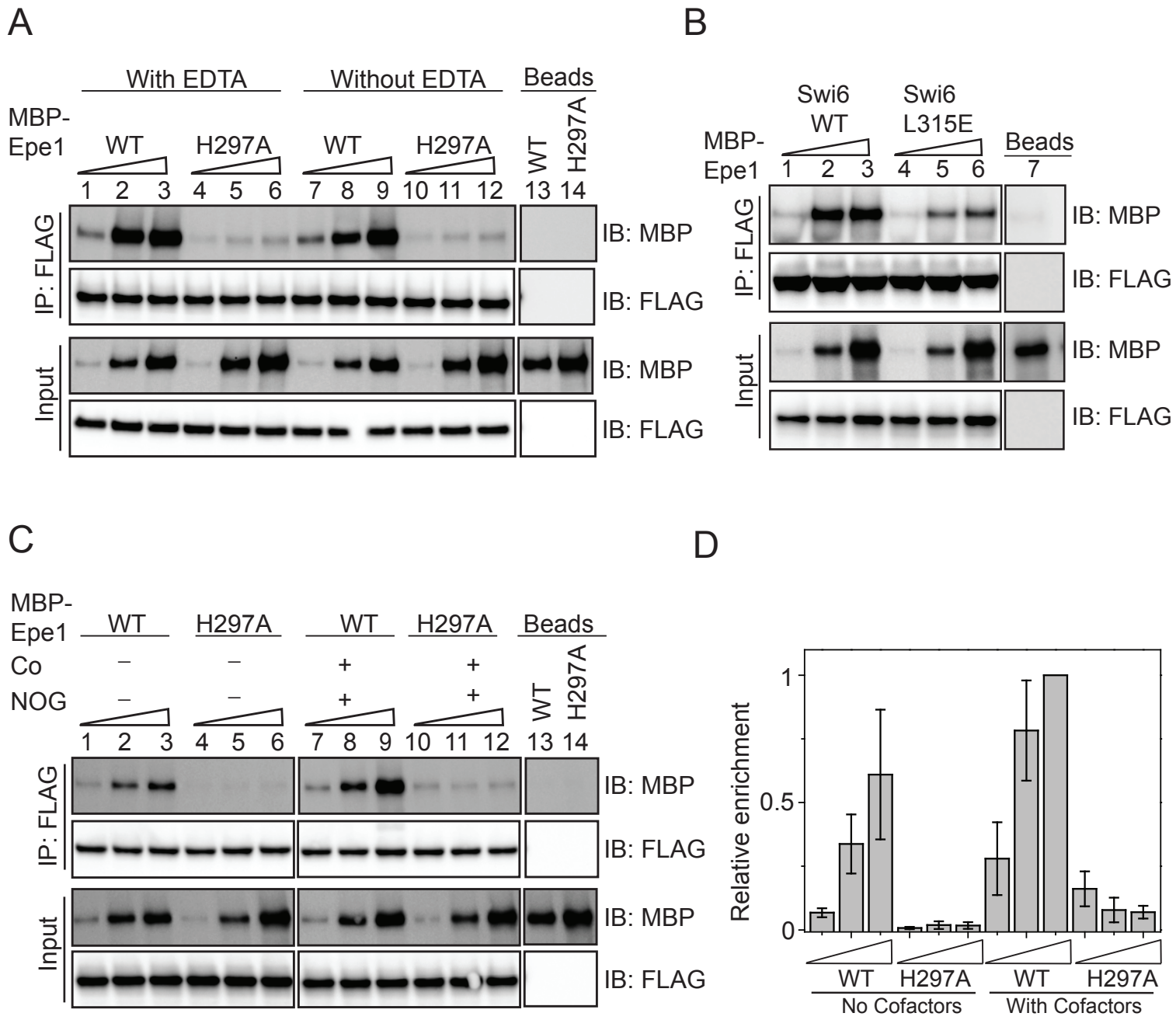
A
With EDTA
Without EDTA
Beads
MBP-Epe1
WT
H297A
WT
H297A
WT
H297A
1 2 3 4 5 6 7 8 9 10 11 12 13 14
IP: FLAG
Input
IB: MBP
IB: FLAG
IB: MBP
IB: FLAG
B
Swi6 WT
Swi6 L315E
MBP-Epe1
Beads
1 2 3 4 5 6 7
IP: FLAG
Input
IB: MBP
IB: FLAG
IB: MBP
IB: FLAG
C
MBP-Epe1
WT
H297A
WT
H297A
Beads
Co
NOG
1 2 3 4 5 6 7 8 9 10 11 12 13 14
IP: FLAG
Input
IB: MBP
IB: FLAG
IB: MBP
IB: FLAG
D
Relative enrichment
1
0.5
0
WT
H297A
WT
H297A
No Cofactors
With Cofactors

Figure 2: *In vitro* binding assays reveal a direct role for the JmjC domain in modulating the interaction between Epe1 and Swi6^{HP1}

A) Western blots of *in vitro* binding assays between recombinant Epe1 and Swi6^{HP1}. Increasing amounts of wild-type MBP-Epe1 and MBP-Epe1 H297A are added while maintaining a fixed amount of 3XFLAG- Swi6^{HP1} on beads. Experiments were performed in the presence and absence EDTA **B)** Western blots reveal that a point mutation in the conserved Swi6^{HP1} chromoshadow domain (Swi6^{HP1}L315E) leads to reduced levels of interaction between Epe1 and Swi6^{HP1}. **C)** Western blots test for the role of co-factors regulating the interaction between Epe1 and Swi6^{HP1}. The addition of co-factor analogs, cobalt and N-oxalyl glycine (NOG) enhances a direct interaction between Epe1 and Swi6^{HP1}. **D)** A quantitative plot of intensities from individual binding experiments reveals an enhancement in the interaction between wild-type Epe1 and Swi6^{HP1} in the presence of co-factors (N=3).

Figure 3

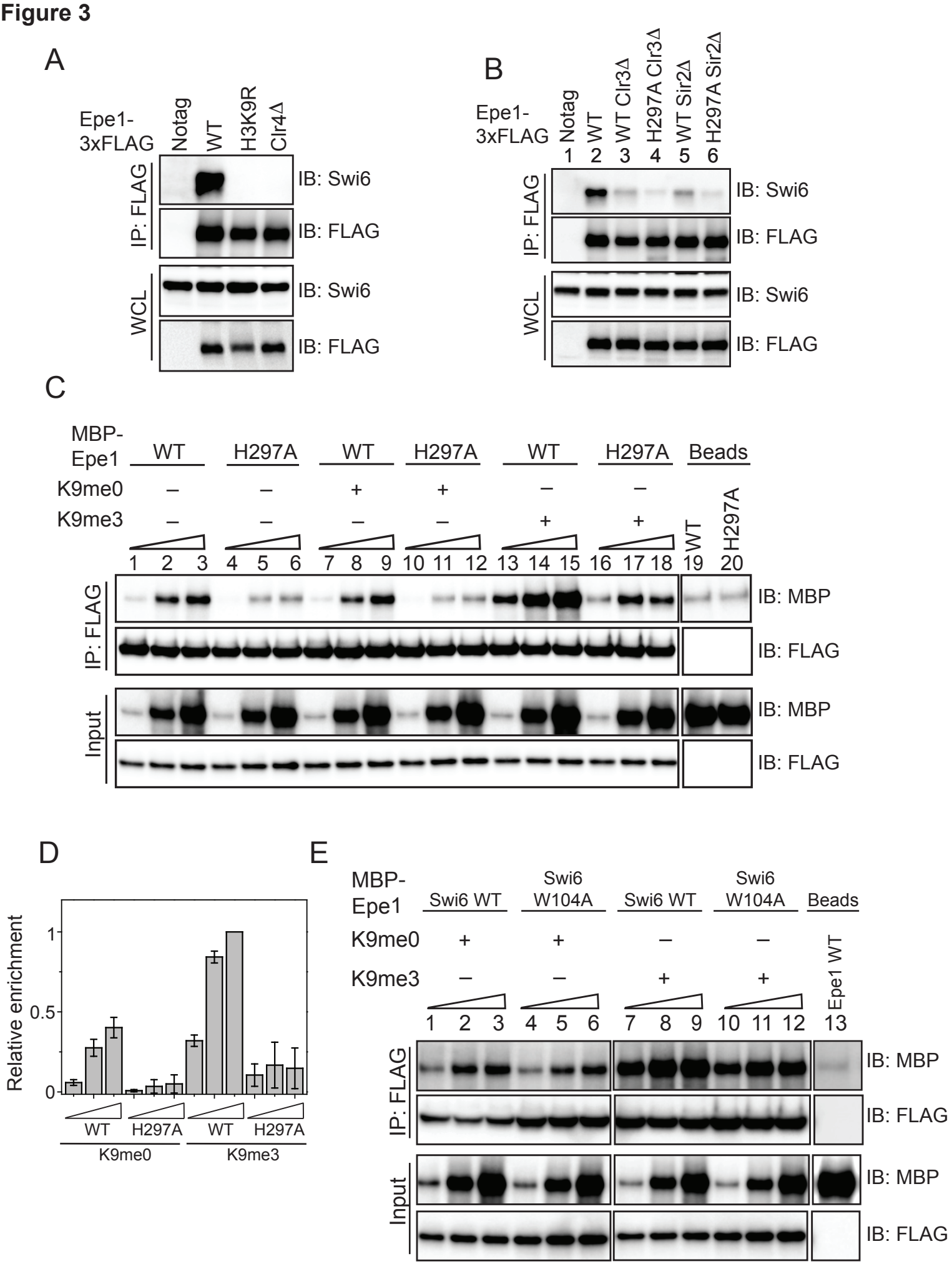
A
Epe1-3xFLAG
Notag
WT
H3K9R
Clr4Δ
IP: FLAG
WCL
IB: Swi6
IB: FLAG
B
Epe1-3xFLAG
Notag
WT
WT Clr3Δ
H297A Clr3Δ
WT Sir2Δ
H297A Sir2Δ
1 2 3 4 5 6
IP: FLAG
WCL
IB: Swi6
IB: FLAG
C
MBP-Epe1
WT
H297A
WT
H297A
WT
H297A
Beads
K9me0
K9me3
1 2 3 4 5 6 7 8 9 10 11 12 13 14 15 16 17 18 19 20
WT
H297A
IP: FLAG
Input
IB: MBP
IB: FLAG
D
Relative enrichment
1
0.5
0
WT
H297A
WT
H297A
K9me0
K9me3
E
MBP-Epe1
Swi6 WT
Swi6 W104A
Swi6 WT
Swi6 W104A
Beads
K9me0
K9me3
1 2 3 4 5 6 7 8 9 10 11 12 13
Epe1 WT
IP: FLAG
Input
IB: MBP
IB: FLAG

Figure 3: H3K9 methylation stimulates complex formation between Epe1 and Swi6^{HP1}

A) Western blots of co-immunoprecipitation measurements reveal the complete absence of an interaction between Epe1-3XFLAG and Swi6^{HP1} in cells which lack H3K9 methylation (*clr4Δ* and H3K9R). **B)** Co-immunoprecipitation measurements reveal that the deletion of histone deacetylases Clr3 or Sir2 which disrupts heterochromatin assembly leads to a concomitant loss of the interaction between Epe1-3XFLAG and Swi6^{HP1}. **C)** Western blots of *in vitro* binding assays between recombinant Epe1 and Swi6^{HP1} in the presence of histone H3 tail peptides (1-21 amino acids). Increasing amounts of wild-type MBP-Epe1 and MBP-Epe1 H297A are added while maintaining a fixed amount of 3XFLAG- Swi6^{HP1} on beads. Experiments were performed in the presence of an unmethylated H3 peptide (H3K9me0) or an H3K9 tri-methylated H3 peptide (H3K9me3). Epe1 exhibits a high affinity state of interaction with Swi6^{HP1} in the presence of a modified histone peptide. **D)** A quantitative plot of intensities from individual binding experiments reveals an enhancement in the interaction between Epe1 and Swi6^{HP1} in the presence of a modified H3K9me3 peptide but no change in the interaction upon addition of an unmodified peptide (N=3). **E)** Western blots of *in vitro* binding assays between recombinant wild-type Epe1 and a Swi6^{HP1} chromodomain mutant, Swi6^{HP1} W104A. The increase in interaction between Epe1 and Swi6^{HP1} in the presence of an H3K9me3 peptide persists in a Swi6^{HP1}W104A CD domain mutant.

Figure 4

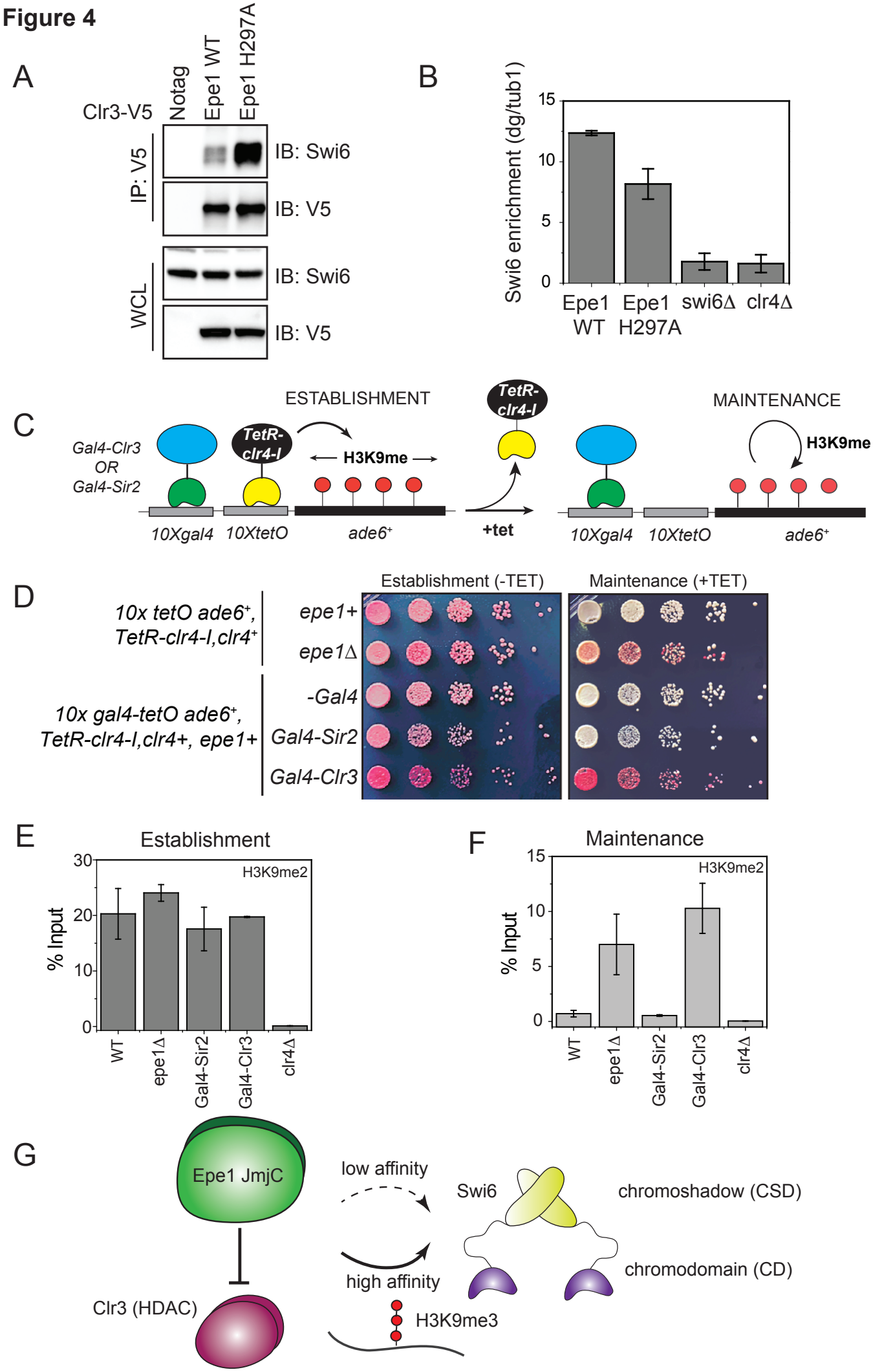
A
Clr3-V5
Notag
Epe1 WT
Epe1 H297A
IP: V5
IB: Swi6
IB: V5
WCL
IB: Swi6
IB: V5
B
Swi6 enrichment (dg/tub1)
15
10
5
0
Epe1 WT
Epe1 H297A
swi6Δ
clr4Δ
C
ESTABLISHMENT
MAINTENANCE
Gal4-Clr3 OR Gal4-Sir2
TetR-clr4-I
H3K9me
+tet
10Xgal4
10XtetO
ade6+
D
Establishment (-TET)
Maintenance (+TET)
10x tetO ade6+, TetR-clr4-I,clr4+
epe1+
epe1Δ
10x gal4-tetO ade6+, TetR-clr4-I,clr4+, epe1+
-Gal4
Gal4-Sir2
Gal4-Clr3
E
Establishment
H3K9me2
% Input
30
20
10
0
WT
epe1Δ
Gal4-Sir2
Gal4-Clr3
clr4Δ
F
Maintenance
H3K9me2
% Input
15
10
5
0
WT
epe1Δ
Gal4-Sir2
Gal4-Clr3
clr4Δ
G
Epe1 JmjC
Clr3 (HDAC)
low affinity
high affinity
Swi6
chromoshadow (CSD)
chromodomain (CD)
H3K9me3

Figure 4: The non-enzymatic function of Epe1 is necessary and sufficient to disrupt epigenetic inheritance

A) Western blots of a co-immunoprecipitation experiment to measure an interaction between Clr3 and Swi6^{HP1}. Clr3-3X V5 tagged exhibits a weak interaction with Swi6^{HP1} in a wild-type Epe1 background which is significantly enhanced in an Epe1 H297A background. **B)** ChIP-qPCR measurements of Swi6^{HP1} occupancy at sites of constitutive heterochromatin formation **C)** A reporter system to detect epigenetic inheritance in the presence of an orthogonal chromatin effector. Heterochromatin initiation depends on TetR-Clr4-I binding (-tetracycline). Orthogonal chromatin effectors can be recruited to the *10xgal4* DNA binding site via a Gal4 DNA binding domain (Gal4 DBD). The addition of tetracycline promotes TetR-Clr4-I dissociation to test for conditions where we can detect initiator independent maintenance of H3K9 methylation in conjunction with an orthogonal chromatin effector. **D)** A color based assay to detect the establishment and maintenance of epigenetic states. The establishment of epigenetic silencing (-tetracycline) results in red colonies. Epigenetic maintenance, indicated by the appearance of red or sectored colonies in +tetracycline medium, depends on the constitutive recruitment of Gal4-Clr3. **E)** ChIP-qPCR measurements of H3K9me2 levels at the ectopic site (*10X tetO ade6*+) during establishment (-tetracycline). (N=2). Error bars represent standard deviations. **F)** ChIP-qPCR measurements of H3K9me2 levels at the ectopic site (*10X tetO ade6*+) during maintenance (+tetracycline) (N=2). Error bars represent standard deviations. **G)** A two-factor authentication model explains how Epe1 disrupts heterochromatin assembly and epigenetic inheritance. Two factors, namely H3K9 methylation and co-factor binding regulate the formation of an inhibitory complex between Epe1 and Swi6^{HP1}which impairs downstream heterochromatin assembly.